A Tropical and Subtropical Land–Sea–Atmosphere Drought Oscillation Mechanism

DORIAN S. ABBOT

School of Engineering and Applied Sciences, Harvard University, Cambridge, Massachusetts

KERRY A. EMANUEL

Program in Atmospheres, Oceans, and Climate, Massachusetts Institute of Technology, Cambridge, Massachusetts

(Manuscript received 26 May 2006, in final form 14 December 2006)

ABSTRACT

A two-column atmospheric model on a land–sea interface is studied. The model has sophisticated convection, cloud, and radiation schemes, a mixed layer ocean, and a bucket model to simulate land hydrology. A self-sustained oscillation in soil moisture with a period on the order of months is found. This oscillation is strongest when the model is run with parameters chosen to correspond to the arid subtropics. The effect of changing model parameters on the oscillation is explored. The existence and qualitative behavior of the oscillation are relatively robust to changes in model parameters.

1. Introduction

A positive feedback between soil moisture anomalies and precipitation has been documented extensively in regional and global climate models (e.g., Walker and Rowntree 1977; Sud and Fennessy 1984; Zheng and Eltahir 1998; Hong and Kalnay 2000; Oglesby and Erickson 1989; Shukla and Mintz 1982). There is observational evidence that such an effect, or at least important parts of it, functions in the climate system (Findell and Eltahir 1997; Betts and Ball 1998; Eltahir 1998; Koster et al. 2003). Analytical and numerical models suggest that this positive feedback should allow some land–atmosphere systems to exist in consistent alternative states with either wet soil and high precipitation or dry soil and low precipitation (Entekhabi et al. 1996, 1992; Rodriguez-Iturbe et al. 1991; Brubaker and Entekhabi 1996). Bimodality in the soil moisture distribution is observed in some regions (D'Odorico and Porporato 2004; D'Odorico et al. 2000; Teuling et al. 2005; Lee and Hornberger 2006), although Teuling et al. (2005) caution that such bimodality can be the result of processes other than the soil moisture–precipitation feedback.

Here we study the behavior of the soil moisture–precipitation feedback in a system with a lower boundary composed of adjacent regions of land and sea. Of particular interest are the ability of this feedback to affect the final state of a land–sea–atmosphere system and whether multiple equilibria such as those found in land–atmosphere systems exist.

There is reason to suspect that feedbacks involving soil moisture may be more complex in a land–sea–atmosphere system than in a land–atmosphere system. For instance, Shukla and Mintz (1982) compared results from an atmospheric general circulation model run for the month of July with evaporation over land set either to zero (dry soil) or to the potential evaporation rate (wet soil). They found that precipitation over land was higher in the wet soil case than in the dry soil case everywhere but in Southeast Asia and India. High land temperatures in the dry soil case caused a thermal low over Southeast Asia and India, which led to increased advection of water vapor from the Indian Ocean and greatly increased precipitation.

This study is conducted using a model consisting of two vertical air columns, one above land and one above ocean. The model's treatment of convection, precipitation, and radiation is sophisticated, but its geometry and treatment of surface hydrology are idealized. We use the model as a tool to gain conceptual understanding of the climate system, rather than for accurate simulation of climate. In this land–sea–atmosphere system,

Corresponding author address: Dorian Abbot, Harvard University, 24 Oxford St., Cambridge, MA 02138.
E-mail: abbot@fas.harvard.edu

DOI: 10.1175/2007JAS2186.1

© 2007 American Meteorological Society

separate and stable drought and pluvial modes for the same external forcing are not found; instead, the model either reaches a constant steady-state soil moisture value regardless of initial conditions, or a self-sustained oscillation in soil moisture develops.

We focus on this soil moisture oscillation. It requires the interaction between the land, ocean, and atmosphere and would not occur if both columns were over either land or ocean. The oscillation operates without a seasonal cycle imposed on the system. It is entirely dependent on the internal dynamics of the system, which involve land soil moisture, evaporation, precipitation, circulation, and advection of atmospheric water vapor.

The model is described in section 2. Results are presented in section 3. A discussion is offered in section 4.

2. Model

The model is two-dimensional in the zonal–height plane. The atmosphere consists of two vertical air columns, similar to that of Nilsson and Emanuel (1999). Each column follows Emanuel and Zivkovic-Rothman (1999). A major difference between this work and that of Nilsson and Emanuel (1999) is that here land is under one column and ocean is under the other, whereas in Nilsson and Emanuel (1999) ocean was under both. Results are presented for a total domain width, including both land and ocean columns, of 1000 km. Qualitatively consistent results are found for domain sizes between 50 and 2000 km. Figure 1 contains a schematic of the model.

The model uses sophisticated schemes for the calculation of convection, clouds, and radiation. The convection scheme is based on Emanuel (1991). The model has a vertical resolution of 25 mb for pressures greater than 100 mb and vertical levels at 80, 60, 40, 30, 25, 20, 15, 10, and 5 mb above this for a total of 46 vertical levels. This is better than the 50-mb resolution necessary for accurate representation of water vapor using this convection scheme (Emanuel and Zivkovic-Rothman 1999). The Bony and Emanuel (2001) cloud parameterization is used. Longwave radiation is calculated using the scheme of Morcrette (1991); shortwave radiation is calculated following Fouquart and Bonnel (1980) and specified to be its annual mean value. Clouds interact fully with radiation.

a. Dynamical equations

The model solves prognostic equations for vorticity, $\eta = u_p - \omega_x$, and meridional momentum, temperature, and specific humidity:

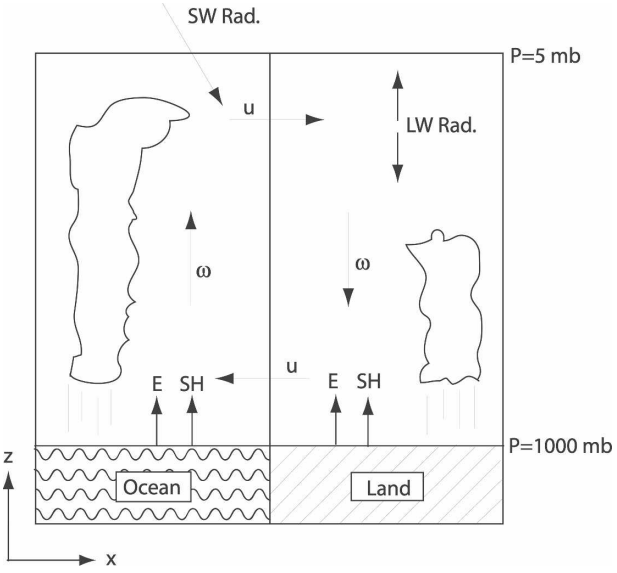

FIG. 1. Schematic of the two-column model in the zonal–height plane. The atmosphere has 46 vertical levels. The model solves nonlinear primitive dynamical equations. Temperature and humidity are computed at each level. The model has a convection scheme based on Emanuel (1991) and uses the Bony and Emanuel (2001) cloud parameterization. Longwave radiation is calculated using the scheme of Morcrette (1991) and incoming shortwave radiation is set to its annual mean value. Clouds interact fully with radiation. The ocean has a mixed layer depth of 70 m and a bucket model is used to simulate land hydrology.

$$\eta_t + u\eta_x + fv_p - \alpha_x = \gamma\eta_{xx} + [\upsilon(p)\eta_p]_p + [f^u_{\text{cnv}}]_p, \tag{1}$$

$$v_t + uv_x + \omega v_p - fu = \gamma v_{xx} + [\upsilon(p)v_p]_p + f^v_{\text{cnv}}, \tag{2}$$

$$T_t + uT_x + \omega T_p = \gamma T_{xx} + \text{SH} + Q + R, \tag{3}$$

$$q_t + uq_x + \omega q_p = \gamma q_{xx} + E + C, \tag{4}$$

where subscripts denote partial derivatives; u and v are the zonal and meridional velocities; T is the temperature; q is the specific humidity; α is the specific volume; f^u_{cnv} and f^v_{cnv} are the time tendencies of zonal and meridional velocity due to convection; SH and E are the sensible heat and evaporative fluxes, which are deposited only into the lowest atmospheric layer; Q represents diabatic heating due to cumulus convection and large-scale condensation; R represents net radiative heating; C represents the moisture source and sink due to cumulus convection and large-scale condensation; and γ is chosen so the damping time scale is 30 day^{-1}. The terms involving $\upsilon(p)$ represent momentum flux convergence in the planetary boundary layer; $\upsilon(p)$ is given by

$$\upsilon(p) = \begin{cases} 100\gamma\left(1 + \dfrac{p - p_s}{\Delta_{\text{pbl}}}\right) & \text{for } p \geq p_s - \Delta_{\text{pbl}}, \\ 0 & \text{for } p < p_s - \Delta_{\text{pbl}}, \end{cases}$$

where p_s is the surface pressure and $\Delta_{\text{pbl}} = 50$ hPa is the pressure scale over which the planetary boundary layer momentum fluxes converge.

Equation (1) is derived from the zonal and vertical momentum equations, neglecting vertical advection of vorticity. Equations (1)–(4) are solved using a leapfrog scheme in time with a Robert filter. Homogeneous Neumann boundary conditions are used.

The specific volume is calculated using the equation of state with a gas constant that includes water vapor effects. The continuity equation is used to define a streamfunction for the zonal and pressure velocities,

$$u = \psi_p,$$

$$\omega = -\psi_y,$$

where ψ is determined by inverting the approximate relationship,

$$\eta \approx \psi_{pp}.$$

b. Heat transport

There is no heat exchange between the ocean and land surfaces, but heat is exchanged between the two columns of air above them by a simple overturning circulation. Because the model exists in the zonal–height plane, it cannot resolve meridional heat transport. In the results presented here the model latitude is typically 25° and does not exceed 35°. Since net meridional heat export occurs at these latitudes in earth's atmosphere, we keep model temperatures from becoming unrealistically high by artificially increasing the surface albedo. This is equivalent to applying a lateral heat transport out of the system at the surface, which is a realistic way of approximating ocean heat transport, but does not accurately account for the vertical structure of atmospheric heat transport.

The annual and zonal mean of the divergence of the northward energy transport at 25° is about 30 W m^{-2} (Fig. 2a of Trenberth and Stepaniak 2003) while the absorbed solar energy flux is about 250 W m^{-2} at 25° (Fig. 1.1 of Gill 1982), so the effect of meridional heat transport at 25° can be approximated by increasing the surface albedo by about 0.10–0.15. Figure 1.3 (b) in Gill (1982) shows that in the vicinity of 25°, ocean albedos are roughly 0.10–0.15 and land albedos are 0.15–0.3 and Table 6.1 in Peixoto and Oort (1992) gives 0.16–0.20 and 0.18–0.28 as reasonable albedos for grassland and sand, respectively. Given these values, the ocean albedo is taken to be 0.25 and the land albedo is taken to be 0.35. The qualitative behavior of the oscillation we present does not depend on these exact albedo choices.

c. Surface and surface fluxes

The ocean and land temperatures are prognostic variables determined by heat balance. The ocean consists of a mixed layer with a uniform temperature and a depth of 70 m. The land surface has a constant volume heat capacity of 2.5×10^6 J m^{-3} K^{-1}, a reasonable value based on Table 10.1 in Peixoto and Oort (1992), and a depth of 1.0 m. The oscillation we present functions when these parameters are varied over two orders of magnitude (section 3d).

Evaporative and sensible heat fluxes are parameterized using bulk aerodynamic formulas, which take the following form over the ocean:

$$E = \rho C_W |\mathbf{v}|[q^*(\text{SST}) - q], \tag{5}$$

$$\text{SH} = \rho C_p C_H |\mathbf{v}|[\text{SST} - \theta]. \tag{6}$$

Here q is the specific humidity, $q^*(T, P)$ is the saturation specific humidity, *SST* is the sea surface temperature, C_p is the heat capacity of air, and $\mathbf{v}$ is the velocity; q, θ, and $\mathbf{v}$ are evaluated at 1000 mb, the lowest model level. We take $C_W = C_H = 1.5 \times 10^{-3}$ over ocean and $C_W = C_H = 3.0 \times 10^{-3}$ over land. Qualitative behavior of the model does not depend on the exact choice of C_W and C_H. The increase in surface fluxes due to convective outflow is included in the model (Emanuel and Zivkovic-Rothman 1999).

Over land, the sensible heat flux is given by simply replacing the sea surface temperature in Eq. (6) with the land surface temperature, T_s. The potential evaporation rate, E_0, is the rate of evaporation that would be expected if the surface were composed of pure water. We calculate E_0 by replacing SST with T_s in Eq. (5).

Since many parameterizations of potential evaporation over land exist, we also tried using that of Hamon (1963), outlined in appendix A of Vorosmarty et al. (1998). Vorosmarty et al. (1998) found that the potential evaporation parameterization of Hamon (1963) performed better than other potential evaporation parameterizations that do not depend on surface cover properties and comparably with surface cover–dependent algorithms. When we used the Hamon (1963) parameterization, we obtained results qualitatively similar to those presented below.

Since the land surface is not composed of pure water, evaporation over land does not in general occur at the potential evaporation rate. In the model, evaporation over land is reduced from the potential evaporation rate by multiplication by a factor between 0 and 1,

$$E_{\text{land}} = f_e E_0,$$

where f_e, the ratio of actual evaporation to potential evaporation, is called the evaporative fraction. If $f_e = 0$,

there is no evaporation from the land regardless of the surface temperature. This would be the case if the land were completely dry and there were no water to evaporate. Alternatively, in a swamp f_e would take the value 1 and evaporation would function as it would over the ocean. Soil type, vegetation type, soil moisture, surface radiation, wind speed, and other parameters affect the ability of the land to evaporate water into the atmosphere and should in principle affect the evaporative fraction. The calculation of f_e is described in the following section.

d. Soil moisture and evaporative fraction

The simple, but standard, bucket model is used to simulate surface hydrology and to calculate evaporative fraction (Manabe 1969). The soil's ability to hold water is measured by the field capacity, W_c, which is the volume of water that can be held per unit surface area. It is measured in meters and can be thought of as the height of the conceptual bucket. An appropriate choice of field capacity depends on soil and vegetation type. For example, the field capacity should be taken to be larger when modeling tropical rain forests than when modeling deserts (Zheng and Eltahir 1998). Typical values of W_c are roughly 0.1–0.5 m (Zheng and Eltahir 1998; Manabe 1969; Robock et al. 1995a). We use a field capacity of 0.10 m. The effects of changing this value are investigated in section 3c.

Soil moisture, like field capacity, is measured in meters. The time tendency of soil moisture, W, is given by the difference between precipitation and evaporation, so long as the soil moisture does not exceed the field capacity,

$$\frac{dW}{dt} = \begin{cases} P - E & \text{for } W < W_c \text{ or } \quad P \le E, \\ 0 & \text{for } W = W_c \text{ and } P > E. \end{cases} \tag{7}$$

By Eq. (8) it is impossible for the soil moisture to become negative. Water is assumed to collect in the soil without running off until the field capacity is reached, at which point excess precipitation becomes runoff and the soil moisture tendency is zero. Manabe (1969) argues that neglecting runoff when the soil moisture does not exceed the field capacity is an approximation that incurs minimal error, except during severe storms.

The bucket model description of soil moisture is simple but physically reasonable. We believe it is an appropriate formulation for our model, which we wish to keep generally applicable and do not intend to use for simulation of a particular region. Furthermore, there is evidence that in some situations more complex soil moisture models do not offer a simulation of soil moisture observations that is superior to the simulation provided by a bucket model (Robock et al. 1995b). Although that study was conducted at midlatitudes rather than the Tropics or subtropics, it implies that the simple bucket model includes the most important aspects of soil moisture dynamics.

Following Manabe (1969), we specify the evaporative fraction to be proportional to soil moisture:

$$f_e = \frac{W}{\alpha W_c}, \tag{8}$$

where $0 < \alpha \le 1$ and f_e has an upper limit of 1. Taking $\alpha < 1$ implies that full evaporation is reached before the land is fully saturated (Manabe 1969; Robock et al. 1995a). Following Zheng and Eltahir (1998), we let $\alpha = 1$. Taking $\alpha = 0.5$ or $\alpha = 0.75$ does not affect the qualitative behavior of the oscillation presented here. Using a smaller α has a similar effect on the oscillation as does reducing the field capacity (section 3c).

Equation (8) describes a scheme for the evaporative fraction that depends directly on soil moisture and indirectly, through the field capacity, on soil and vegetation type. The scheme does not have a canopy model and neglects many of the complexities of evapotranspiration. We leave further discussion of the advantages and limitations of this evaporative fraction scheme for section 4.

3. Results

The model exhibits behavior that can be classified into two regimes. In the first the soil moisture approaches a constant at long times. In the second there is a self-sustained oscillation in soil moisture at long times. In both regimes the final solution is independent of initial conditions. Some examples of the former regime will be discussed in sections 3b and 3e. The latter regime is the focus of this work.

a. Soil moisture oscillation

Oscillations in land soil moisture occur when the model is run at a wide range of latitudes, field capacities, and surface albedos. Three sample cycles of an oscillation are shown in Fig. 2. Here the latitude is 25°, the land albedo is 0.35, and the field capacity is 0.10 m. These choices are consistent with a semiarid subtropical region. The oscillation is self-sustained and, in addition to the soil moisture, involves the circulation, convection, and precipitation. It is not perfectly periodic, but a measure of the period will be discussed below. A similar oscillation results regardless of the initial conditions from which the model is started.

We will now proceed with a physical description of

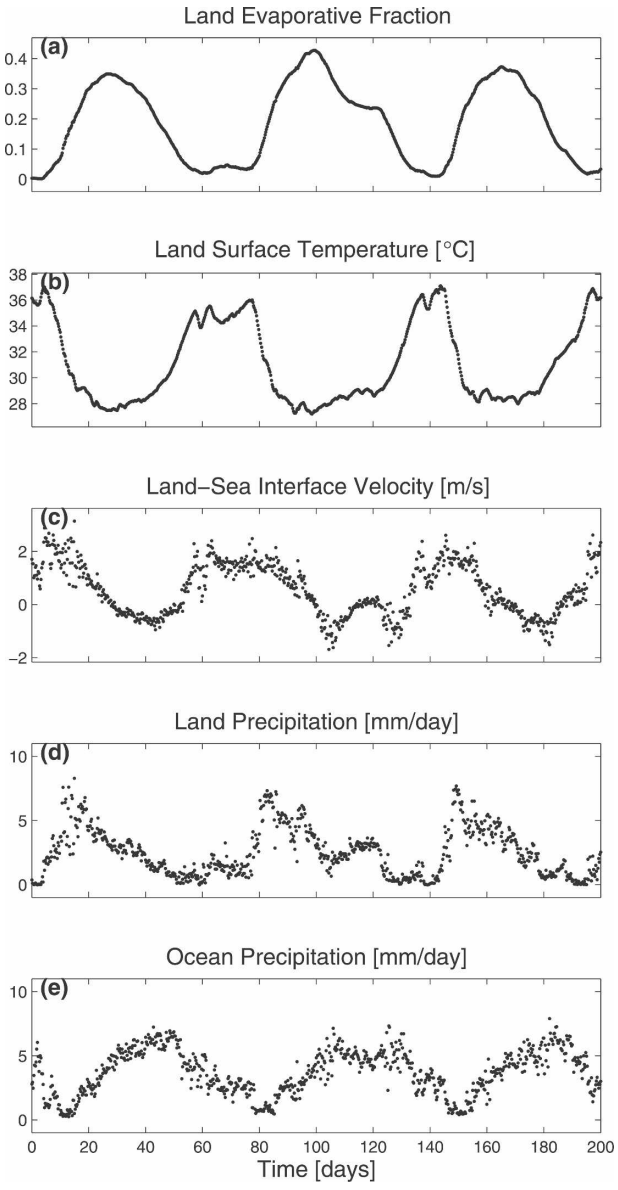

FIG. 2. A 200-day sample time series of important diagnostics from the model. Points represent values every 6 h. The model is run at 25° lat with a land albedo of 0.35 and a field capacity of 0.10 m. (a) Land evaporative fraction, which is proportional to the soil moisture [Eq. (8)], (b) land surface temperature, (c) surface velocity at the land–sea interface (positive is toward the land), (d) precipitation over the land column, and (e) precipitation over the ocean column.

the progression of a cycle starting from a minimum in soil moisture. The minimum in soil moisture corresponds to a minimum in evaporative fraction and latent heat flux, and a maximum in the Bowen ratio. As the ability of the land to lose heat by evaporation is greatly reduced or shut off completely, the land surface temperature increases dramatically. The increase in land surface temperature causes low-level ascent over land, which reverses the land–sea interface velocity so that it blows landward at the surface, advecting moisture evaporated from the sea surface over the land column. This moisture increases the moist static energy of the land boundary layer, destabilizing the column and causing deep convection, by which the moisture is lifted, condenses, and precipitates. At this point there is ascent over the land and descent over the ocean at all vertical levels. The precipitation over land slowly increases the land soil moisture. As the soil moisture increases and the land is again able to lose heat by evaporation, the land surface temperature drops, causing the circulation to begin to change direction. As a result, by the time the soil moisture has reached a maximum the circulation has switched direction, ascending over the ocean and descending over the land. This shuts off the advection of moisture from the ocean to the land and consequently shuts off deep convection over the land. With no deep convection and precipitation over the land the soil moisture begins to decrease until it reaches its minimum and the cycle repeats itself.

This mechanism depends crucially on the advection of low-level moisture by the sea breeze. When intercolumn advection of moisture is turned off in the code, no oscillation occurs and the system quickly reverts to a state with no land soil moisture and no precipitation over land. The importance of the advection of moisture between columns can be seen in Figs. 2c–e. Positive values of the land–sea interface velocity cause increased precipitation over land and decreased precipitation over ocean, as a result of landward advection of moisture. The reverse is true as well.

Although the soil moisture oscillation is not perfectly periodic, it is important to get a measure of its period. For this, we calculate the first moment of the power spectral density (PSD) of the soil moisture time series:

$$\overline{\omega} = \frac{2\pi}{T} = \frac{\int_0^\infty \omega P(\omega)\, d\omega}{\int_0^\infty P(\omega)\, d\omega}, \tag{9}$$

where T denotes the period. In Eq. (9), $P(\omega)$ is the PSD calculated on the last 6000 days of 8000-day model runs using the multitaper method with 10 degrees of freedom. The resulting period is insensitive to both the initial length of time allowed for transients to die down and the number of degrees of freedom used. This method yields an average period of 82 days for the oscillation presented in this section.

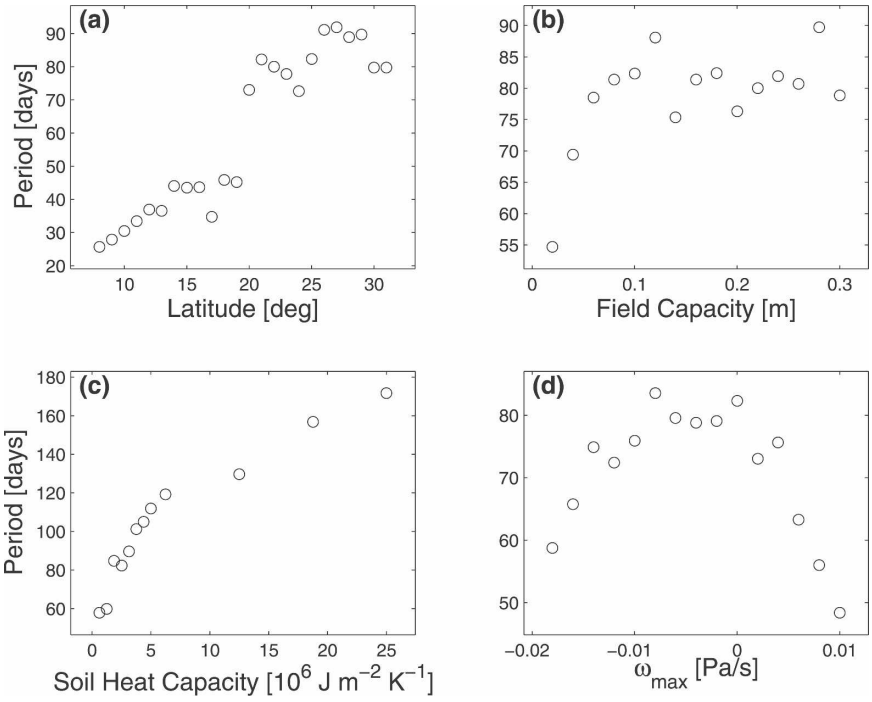

FIG. 3. Period of soil moisture oscillation when important model parameters are varied. The varied parameter is (a) lat, (b) soil field capacity, (c) soil heat capacity, and (d) applied pressure velocity. In (b)–(d) the lat is 25°.

b. *Varying the latitude*

Figure 3a shows the period of oscillation as a function of latitude. There is a general upward trend in the period as the latitude is increased, although this trend is not monotonic. Near the equator evaporation from the ocean is high because the SST is high. This moistens the system as a whole, leads to high precipitation over both ocean and land, and drives the soil moisture to the field capacity. Poleward of about 33° the ocean temperature and evaporation from the ocean are low enough that there is not enough moisture in the air above the ocean to be advected over the land and destabilize the column. Consequently the soil moisture level stays near zero and no oscillation occurs.

Similar experiments varying only the incoming shortwave radiation or Coriolis parameter with latitude show that the change of behavior as the latitude is varied is due mainly to decreased solar radiation at higher latitudes (not shown). This implies that the primary reason the period of oscillation increases with latitude is that the land takes longer to heat up at the stage in the oscillation when the evaporative fraction is zero at lower solar forcing (cf. with section 3d).

c. *Effect of the field capacity*

In Fig. 2a the amplitude of oscillation of the evaporative fraction around its mean value is about 0.2. This corresponds to an amplitude of oscillation of the soil moisture of about 0.02 m [Eq. (8)]. As the field capacity is changed, this amplitude stays roughly constant. For field capacities lower than about 6 cm the evaporative fraction varies between 0 and nearly 1, so that as the field capacity is increased, a larger variation of soil moisture is required for the same variation in evaporative fraction. This leads to the period of oscillation increasing as the field capacity increases (Fig. 3b). At higher field capacities, the amplitude of oscillation of the evaporative fraction decreases as the field capacity is increased, but amplitude of oscillation of the soil moisture and the period stay roughly constant (Fig. 3b).

d. *Effect of soil heat capacity*

Since the oscillation mechanism requires variations in the surface temperature, here we investigate the effect of soil heat capacity on it. We find that the basic behavior of the oscillation is robust to increasing and decreasing the soil heat capacity by an order of magnitude. Figure 3c shows the period of oscillation as a function of the land heat capacity. Increasing the heat capacity elongates the response time of the land temperature changes and so increases the period of oscillation. Increasing land heat capacity also smoothes the land temperature time series and leads to more regular cycles. Changing the heat capacity does not have a large

effect on the amplitude of the surface temperature oscillation.

In principle the soil heat capacity should depend on the amount of soil moisture. However, the amount of soil moisture that can vary is only a fraction of the total soil moisture (Robock et al. 1995a)—the rest is locked in the soil. This means that the heat capacity of the soil should have only a small dependence on the soil moisture. For example, if the field capacity of the soil is 0.1 m, then the variable soil moisture can change the heat capacity of the soil per unit surface area by 4.19×10^5 J m^{-2}, or roughly one-fifth of the standard value adopted for these runs. Since varying the heat capacity over two orders of magnitude did not disrupt the oscillation mechanism presented here, we believe it is unlikely that such small time-dependent variations in the heat capacity would.

e. Adding descent

Since large-scale vertical motion associated with the Hadley circulation is a characteristic of the seasonal average climatology in the Tropics and subtropics, we here investigate the effects of applied ascent and descent on the oscillation mechanism. To do this we apply a pressure velocity to both columns that is parabolic in pressure, following Eq. (33) in Emanuel (1991):

$$\omega = 4\omega_{\max} \frac{(p_0 - p)(p - p_1)}{(p_0 - p_1)^2}. \tag{10}$$

We tested maximum applied pressure velocities, $\omega_{\max}$, ranging from -0.04 to 0.04 Pa s^{-1}. The observed zonally and seasonally averaged pressure velocities fall within this range (Peixoto and Oort 1992).

Large-scale descent inhibits convection, while ascent aids it. For $\omega_{\max}$ less than -0.02 Pa s^{-1} there is always strong convection and precipitation over land and the land evaporative fraction stays near one. For $\omega_{\max}$ greater than 0.01 Pa s^{-1}, there is little or no precipitation and the soil moisture goes to zero.

A soil moisture oscillation occurs for -0.02 Pa $s^{-1} \leq \omega_{\max} \leq 0.01$ Pa s^{-1}. The period is plotted as a function of $\omega_{\max}$ in Fig. 3d. As descent is increased, the soil moisture oscillation has reduced mean and amplitude (not shown). The reduction in amplitude leads to a reduction in period. For -0.02 Pa $s^{-1} \leq \omega_{\max} \leq -0.01$ Pa s^{-1} there is a similar reduction in amplitude and period as ascent is increased, although the mean soil moisture increases. Ascent has little affect on the oscillation for -0.01 Pa $s^{-1} \leq \omega_{\max} \leq 0.0$ Pa s^{-1}.

The soil moisture oscillation mechanism is robust to moderate large-scale ascent and descent. In the latitude range 20°–30°, where the soil moisture oscillations are strongest, the zonal and seasonal average pressure velocity only exceeds the range in which oscillations occur during descent of the Hadley cell during boreal winter. It is possible that local values of vertical motion could be large enough to disrupt soil moisture oscillations in certain regions.

f. Adding more columns

An important test of the robustness of the proposed mechanism is whether it functions at higher zonal resolution. To investigate this we increased the total number of columns to 16, with 8 over land and 8 over ocean. We dealt with surface hydrology in two ways. First, we placed a bucket model under each atmospheric column over land and assumed that all runoff flowed directly into the ocean, instead of into adjacent columns. This is equivalent to assuming the runoff flows relatively quickly into rivers that carry it to the sea. Second, we placed only one soil moisture bucket for the entire land surface. We found similar results using both methods, which indicates that the mechanism can operate regardless of the specific drainage patterns of the land region.

Sample cycles of the soil moisture oscillation when the zonal resolution is increased to 16 columns and 8 individual soil moisture buckets are used are displayed in Fig. 4. All parameters except number of columns are as in section 2a and Fig. 2. In Fig. 4 the evaporative fraction, precipitation, and surface temperature are averages over the eight land or ocean columns. The land–sea interface surface velocity is an average of the interface velocities for the three land and three ocean columns surrounding the land–sea interface. An oscillation that functions in the same way as that displayed in Fig. 2 is evident.

4. Discussion

We have identified a mechanism through which an oscillation in soil moisture in coastal regions of the Tropics and subtropics may result. We investigated this oscillation using a sophisticated radiative-convective model with an idealized geometry. It is self-sustained and independent of initial conditions. It does not require seasonal forcing; it is due entirely to the internal dynamics of the system. The oscillation operates on a variety of spatial and temporal scales and is able to function in a qualitatively similar way for a large range of parameters.

Understanding the role of soil moisture in the climate system may help extend the range and increase the accuracy of climate forecasts (Koster et al. 2004; Beljaars et al. 1996). Soil moisture may also play an important role in monsoons. For instance, Webster (1983) and Srinivasan et al. (1993) find that soil moisture is impor-

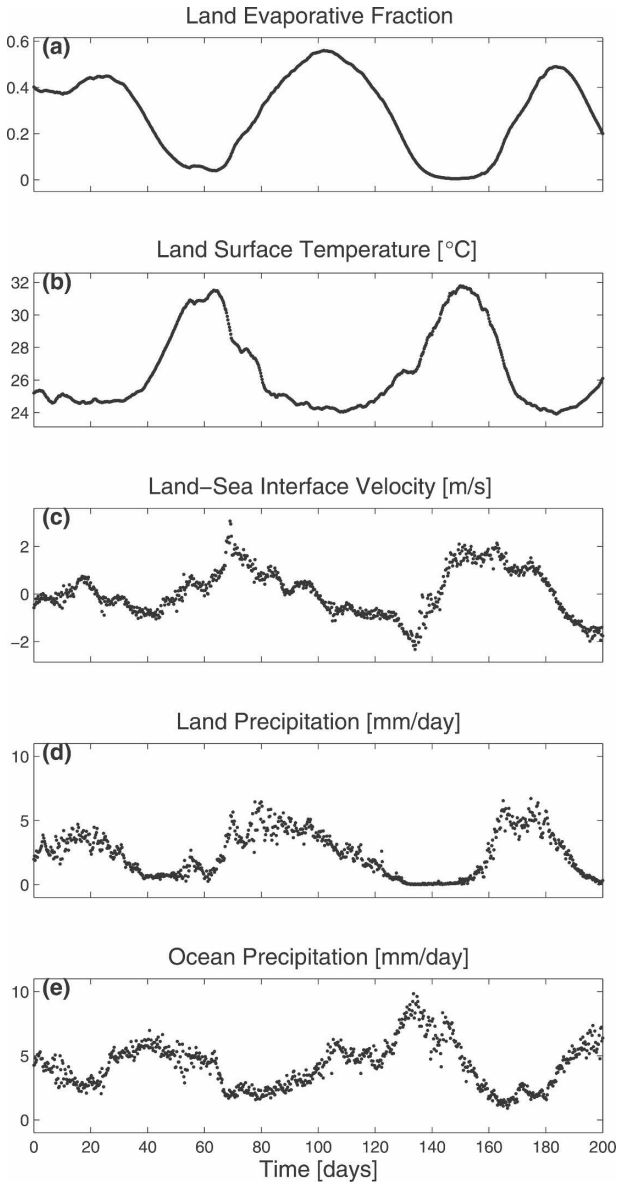

FIG. 4. Results of a run with 16 total columns, 8 over land and 8 over ocean. Other parameters and figure layout are as in Fig. 2. Points represent the mean over either land or ocean, except in the case of the land–sea interface velocity, which is an average of the interface velocities for the 3 land and 3 ocean columns surrounding the land–sea interface.

tant for the propagation across the land of maximal monsoonal convective activity, although Ferranti et al. (1999) dispute this conclusion. However, Ferranti et al. (1999) find that soil moisture plays a role in determining the low-frequency intraseasonal monsoon variability and is therefore important for interannual monsoon prediction.

In this work we have neglected the effect of soil moisture on surface albedo and any resulting feedback (Charney et al. 1977). Including this effect in our model could reduce the amplitude of the oscillation, since an increase in surface temperature when the land is dry is crucial for it to function and drier soil tends to have a higher albedo.

We have used standard, but relatively simple, formulations of the potential evaporation and evaporative fraction over land in this model. We use a bulk aerodynamic formula to calculate the potential evaporation and a bucket model to calculate soil moisture and evaporative fraction. This method allows only a perfunctory simulation of the dependence of evaporation on surface cover and vegetation characteristics through the field capacity. Including a canopy model and a more detailed land hydrology model could potentially alter the oscillation found here. However, the main qualitative feature of evaporation necessary for the oscillation we present to function is that evaporation be low when the soil is relatively dry and high when the soil is relatively wet (section 3a). We expect this behavior to be robust. We believe the modeling choices we have made are appropriate for a conceptual model and derive confidence in our results from the robustness of these results to large changes in model parameters (sections 3b–e) and to the substitution of an alternative potential evaporation parameterization over land (section 2c).

We have not included weather, a diurnal cycle, or an annual cycle in this model. While these effects are likely to be less important in the Tropics and subtropics than in the midlatitudes, they could be potentially disruptive to the oscillation we have found.

We have found a potentially interesting phenomenon using a simple model and have offered a physical and dynamically consistent description of it. However, the soil moisture oscillation we present should not be viewed as a simulation of climate behavior in a particular region. This oscillation should be investigated using a more comprehensive model before its relevance can be established.

Acknowledgments. The authors gratefully acknowledge useful conversations with Peter Huybers and the helpful comments of two anonymous reviewers on an early version of this paper. DA was supported by an NDSEG fellowship, sponsored by the Department of Defense. This work was partially supported by the NSF paleoclimate program, ATM-0502482.

REFERENCES

Beljaars, A. C. M., P. Viterbo, M. J. Miller, and A. K. Betts, 1996: The anomalous rainfall over the United States during July

1993: Sensitivity to land surface parameterization and soil moisture anomalies. *Mon. Wea. Rev.,* **124,** 362–383.

Betts, A. K., and J. H. Ball, 1998: FIFE surface climate and site-average dataset 1987–89. *J. Atmos. Sci.,* **55,** 1091–1108.

Bony, S., and K. A. Emanuel, 2001: A parameterization of the cloudiness associated with cumulus convection; evaluation using TOGA COARE data. *J. Atmos. Sci.,* **58,** 3158–3183.

Brubaker, K. L., and D. Entekhabi, 1996: Analysis of feedback mechanisms in land-atmosphere interaction. *Water Resour. Res.,* **32,** 1343–1357.

Charney, J., W. J. Quirk, S. H. Chow, and J. Kornfield, 1977: A comparative study of the effects of albedo change on drought in semi-arid regions. *J. Atmos. Sci.,* **34,** 1366–1385.

D'Odorico, P., and A. Porporato, 2004: Preferential states in soil moisture and climate dynamics. *Proc. Natl. Acad. Sci. USA,* **101,** 8848–8851.

——, L. Ridolfi, A. Porporato, and I. Rodriguez-Iturbe, 2000: Preferential states of seasonal soil moisture: The impact of climate fluctuations. *Water Resour. Res.,* **36,** 2209–2219.

Eltahir, E. A. B., 1998: A soil moisture-rainfall feedback mechanism. 1. Theory and observations. *Water Resour. Res.,* **34,** 765–776.

Emanuel, K. A., 1991: A scheme for representing cumulus convection in large-scale models. *J. Atmos. Sci.,* **48,** 2313–2335.

——, and M. Zivkovic-Rothman, 1999: Development and evaluation of a convection scheme for use in climate models. *J. Atmos. Sci.,* **56,** 1766–1782.

Entekhabi, D., I. Rodriguez-Iturbe, and R. L. Bras, 1992: Variability in large-scale water balance with land surface-atmosphere interaction. *J. Climate,* **5,** 798–813.

——, ——, and F. Castelli, 1996: Mutual interaction of soil moisture state and atmospheric processes. *J. Hydrol.,* **184** (1–2), 3–17.

Ferranti, L., J. M. Slingo, T. N. Palmer, and B. J. Hoskins, 1999: The effect of land-surface feedbacks on the monsoon circulation. *Quart. J. Roy. Meteor. Soc.,* **125,** 1527–1550.

Findell, K. L., and E. A. B. Eltahir, 1997: An analysis of the soil moisture-rainfall feedback, based on direct observations from Illinois. *Water Resour. Res.,* **33,** 725–735.

Fouquart, Y., and B. Bonnel, 1980: Computations of solar heating of the earth's atmosphere: A new parameterization. *Beitr. Phys. Atmos.,* **53,** 35–62.

Gill, A. E., 1982: *Atmosphere–Ocean Dynamics.* Academic Press, 662 pp.

Hamon, W. R., 1963: Computation of direct runoff amounts from storm rainfall. *Int. Assoc. Sci. Hydrol. Publ.,* **63,** 52–62.

Hong, S. Y., and E. Kalnay, 2000: Role of sea surface temperature and soil-moisture feedback in the 1998 Oklahoma-Texas drought. *Nature,* **408,** 842–844.

Koster, R. D., M. J. Suarez, R. W. Higgins, and H. M. Van den Dool, 2003: Observational evidence that soil moisture variations affect precipitation. *Geophys. Res. Lett.,* **30,** 1241, doi:10.1029/2002GL016571.

——, and Coauthors, 2004: Regions of strong coupling between soil moisture and precipitation. *Science,* **305,** 1138–1140.

Lee, T. R., and G. M. Hornberger, 2006: Inferred bimodality in the distribution of soil moisture at Big Meadows, Shenandoah National Park, Virginia. *Geophys. Res. Lett.,* **33,** L06407, doi:10.1029/2005GL025536.

Manabe, S., 1969: Climate and the ocean circulation. *Mon. Wea. Rev.,* **97,** 739–774.

Morcrette, J.-J., 1991: Radiation and cloud radiative properties in the European Center for Medium Range Weather Forecasts forecasting system. *J. Geophys. Res.,* **96,** 9121–9132.

Nilsson, J., and K. A. Emanuel, 1999: Equilibrium atmospheres of a two-column radiative-convective model. *Quart. J. Roy. Meteor. Soc.,* **125,** 2239–2264.

Oglesby, R. J., and D. J. Erickson III, 1989: Soil moisture and the persistence of North American drought. *J. Climate,* **2,** 1362–1380.

Peixoto, J. P., and A. H. Oort, 1992: *Physics of Climate.* American Institute of Physics, 520 pp.

Robock, A., K. Y. Vinnikov, C. A. Schlosser, N. A. Speranskaya, and Y. Xue, 1995a: Use of midlatitude soil moisture and meteorological observations to validate soil moisture simulations with biosphere and bucket models. *J. Climate,* **8,** 15–35.

Rodriguez-Iturbe, I., D. Etekhabi, and R. Bras, 1991: Nonlinear dynamics of soil moisture at climate scales. 1. Stochastic analysis. *Water Resour. Res.,* **27,** 1899–1906.

Shukla, J., and Y. Mintz, 1982: Influence of land-surface evapotranspiration on the Earth's climate. *Science,* **215,** 1498–1501.

Srinivasan, J., S. Gadgil, and P. J. Webster, 1993: Meridional propagation of large-scale monsoon convective zones. *Meteor. Atmos. Phys.,* **52** (1–2), 15–35.

Sud, Y. C., and M. J. Fennessy, 1984: Influence of evaporation in semi-arid regions on the July circulation: A numerical study. *J. Climatol.,* **4,** 383–398.

Teuling, A. J., R. Uijlenhoet, and P. A. Troch, 2005: On bimodality in warm season soil moisture observations. *Geophys. Res. Lett.,* **32,** L13402, doi:10.1029/2005GL023223.

Trenberth, K. E., and D. P. Stepaniak, 2003: Covariability of components of poleward atmospheric energy transports on seasonal and interannual timescales. *J. Climate,* **16,** 3691–3705.

Vorosmarty, C. J., C. A. Federer, and A. L. Schloss, 1998: Potential evaporation functions compared on U.S. watersheds: Possible implications for global-scale water balance and terrestrial ecosystem modeling. *J. Hydrol.,* **207** (3–4), 147–169.

Walker, J., and P. R. Rowntree, 1977: The effect of soil-moisture on circulation and rainfall in a tropical model. *Quart. J. Roy. Meteor. Soc.,* **103,** 29–46.

Webster, P. J., 1983: Mechanisms of monsoon low-frequency variability: Surface hydrological effects. *J. Atmos. Sci.,* **40,** 2110–2124.

Zheng, X. Y., and E. A. B. Eltahir, 1998: A soil moisture-rainfall feedback mechanism. 2. Numerical experiments. *Water Resour. Res.,* **34,** 777–785.